Experimental demonstration of 30 Gb/s direct-detection optical OFDM transmission with blind symbol synchronisation using virtual subcarriers

R. Bouziane,[1,*] P. A. Milder,[2] S. Erkılınç,[1] L. Galdino,[1] S. Kilmurray,[1] B. C. Thomsen,[1] P. Bayvel,[1] and R. I. Killey[1]

[1]*Optical Networks Group, Department of Electronic and Electrical Engineering, University College London (UCL), Torrington Place, London WC1E 7JE, UK*

[2]*Department of Electrical and Computer Engineering, Stony Brook University, Light Engineering 231, Stony Brook, NY 11794, USA*

[*]*r.bouziane@ucl.ac.uk*

Abstract: The paper investigates the performance of a blind symbol synchronisation technique for optical OFDM systems based on virtual subcarriers. The test-bed includes a real-time 16-QAM OFDM transmitter operating at a net data rate of 30.65 Gb/s using a single OFDM band with a single FPGA-DAC subsystem and demonstrates transmission over 23.3 km SSMF with direct detection at a BER of 10^{-3}. By comparing the performance of the proposed synchronisation scheme with that of the Schmidl and Cox algorithm, it was found that the two approaches achieve similar performance for large numbers of averaging symbols, but the performance of the proposed scheme degrades as the number of averaging symbols is reduced. The proposed technique has lower complexity and bandwidth overhead as it does not rely on training sequences. Consequently, it is suitable for implementation in high speed optical OFDM transceivers.

OCIS codes: (060.2330) Fiber optics communications; (060.4080) Modulation.

References and links

1. N. Cvijetic, "OFDM for next-generation optical access networks," J. Lightwave Technol. **30**(4), 384–398 (2012).
2. Y. Benlachtar, R. Bouziane, R. I. Killey, C. Berger, P. A. Milder, R. Koutsoyannis, J. C. Hoe, M. Püschel, and M. Glick, "Optical OFDM for the data center," in *Proc. International Conference on Transparent Optical Networks (ICTON 2010)*, paper We.A4.3.
3. T. M. Schmidl and D. C. Cox, "Robust frequency and timing synchronization for OFDM," IEEE Trans. Commun. **45**(12), 1613–1621 (1997).
4. R. P. Giddings and J. M. Tang, "Real-Time experimental demonstration of a versatile optical OFDM symbol synchronization technique using low-power DC offset signalling," in *Proc. European Conference and Exhibition on Optical Communication (ECOC 2011)*, paper We.9.A.3.
5. X. Q. Jin, R. P. Giddings, E. Hugues-Salas, and J. M. Tang, "Real-time experimental demonstration of optical OFDM symbol synchronization in directly modulated DFB laser-based 25km SMF IMDD systems," Opt. Express **18**(20), 21100–21110 (2010).
6. R. Bouziane, Y. Benlachtar, and R. I. Killey, "Frequency-based frame synchronization for high-speed optical OFDM," in *Proc. Photonics in Switching Conference* (2012), paper Th-S15-O12.
7. R. Bouziane, R. Schmogrow, D. Hillerkuss, P. A. Milder, C. Koos, W. Freude, J. Leuthold, P. Bayvel, and R. I. Killey, "Generation and transmission of 85.4 Gb/s real-time 16QAM coherent optical OFDM signals over 400 km SSMF with preamble-less reception," Opt. Express **20**(19), 21612–21617 (2012).
8. R. Bouziane, "OFDM symbol synchronization based on virtual subcarriers," in *Proc. IEEE Photonics Conference* (2013), paper MG1.4.
9. R. Bouziane, P. A. Milder, S. Kilmurray, B. C. Thomsen, S. Pachnicke, P. Bayvel, and R. I. Killey, "Blind symbol synchronisation in direct-detection optical OFDM using virtual subcarriers," in *Proc. Optical Fiber Communication Conference*, OSA Technical Digest (Optical Society of America, 2014), paper Th3K.5.
10. H. Liu and U. Tureli, "A high-efficiency carrier estimator for OFDM communications," IEEE Commun. Lett. **2**(4), 104–106 (1998).
11. U. Tureli, H. Liu, and M. D. Zoltowski, "OFDM blind carrier offset estimation: ESPRIT," IEEE Trans. Commun. **48**(9), 1459–1461 (2000).

#203554 - $15.00 USD Received 20 Dec 2013; revised 31 Jan 2014; accepted 31 Jan 2014; published 18 Feb 2014

12. X. Ma, C. Tepedelenlioglu, G. B. Giannakis, and S. Barbarossa, "Non-data-aided carrier offset estimators for OFDM with null subcarriers: identifiability, algorithms, and performance," IEEE J. Sel. Areas Comm. **19**(12), 2504–2515 (2001).
13. D. Huang and K. B. Letaief, "Carrier frequency offset estimation for OFDM systems using null sub-carriers," IEEE Trans. Commun. **54**(5), 813–823 (2006).
14. E. Hugues-Salas, R. P. Giddings, X. Q. Jin, J. L. Wei, X. Zheng, Y. Hong, C. Shu, and J. M. Tang, "Real-time experimental demonstration of low-cost VCSEL intensity-modulated 11.25 Gb/s optical OFDM signal transmission over 25 km PON systems," Opt. Express **19**(4), 2979–2988 (2011).
15. J. Tang, E. Hugues-Salas, and R. Giddings, "First experimental demonstration of real-time adaptive transmission of 20Gb/s dual-band optical OFDM signals over 500m OM2 MMFs," in *Proc. Optical Fiber Communication Conference*, OSA Technical Digest (Optical Society of America, 2013), paper OTh3A.1.
16. S. Cho, K. W. Doo, J. H. Lee, J. Lee, S. I. Myong, and S. S. Lee, "Demonstration of a real-time 16 QAM encoded 11.52 Gb/s OFDM transceiver for IM/DD OFDMA-PON systems," in *Proc. 18th OptoElect. And Comm. Conf. (OECC)*, Kyoto, Japan (2013), Paper WP2-3.
17. D. Qian, T. T.-O. Kwok, N. Cvijetic, J. Hu, and T. Wang, "41.25 Gb/s real-time OFDM receiver for variable rate WDM-OFDMA-PON transmission," in *Proc. Optical Fiber Communication Conference*, OSA Technical Digest (Optical Society of America, 2010), paper PDPD9.
18. R. P. Giddings, E. Hugues-Salas, and J. M. Tang, "30Gb/s real-time triple sub-band OFDM transceivers for future PONs beyond 10Gb/s/λ," in *Proc. European Conference and Exhibition on Optical Communication* (2013), paper P.6.7.
19. F. Li, X. Xiao, X. Li, and Z. Dong, "Real-time demonstration of DMT-based DDO-OFDM transmission and reception at 50Gb/s," in *Proc. European Conference and Exhibition on Optical Communication* (2013), paper P.6.13.
20. P. Milder, F. Franchetti, J. C. Hoe, and M. Püschel, "Computer generation of hardware for linear digital signal processing transforms," ACM Trans. Des. Autom. Electron. Syst. **17**(2), 1–33 (2012).
21. F. Chang, K. Onohara, and T. Mizuochi, "Forward error correction for 100 G transport networks," IEEE Commun. Mag. **48**(3), S48–S55 (2010).
22. N. Kaneda, Y. Qi, L. Xiang, S. Chandrasekhar, W. Shieh, and Y. Chen, "Real-time 2.5 GS/s coherent optical receiver for 53.3-Gb/s sub-banded OFDM," J. Lightwave Technol. **28**(4), 494–501 (2010).

1. Introduction

Direct-detection optical orthogonal frequency division multiplexing (DD-OFDM) has been suggested as a potentially attractive technology for future passive optical networks (PON), data centres, and back-haul links [1,2]. In addition to its spectral efficiency and efficient dispersion compensation, OFDM and orthogonal frequency division multiple access (OFDMA) offer flexible and efficient frequency-domain allocation of bandwidth resources by allowing multiple users to share the bandwidth with fine granularity [1].

Symbol synchronisation, which is the process of aligning the receiver fast Fourier transform (FFT) with the transmitter inverse FFT (IFFT), is one of the major components in the OFDM transceiver design. The signal detected at the receiver is a series of symbols with no distinctive boundaries between them. The receiver must identify these symbol boundaries correctly before processing them, otherwise the FFT would process samples from adjacent symbols causing inter-symbol interference and bit error ratio (BER) degradation. Amongst the several methods that have been proposed for symbol synchronisation in wireless systems is the well-known Schmidl and Cox (S&C) algorithm [3]. However, direct implementation of this method in high speed optical communications is computationally expensive because of the high sampling frequency required in such systems (multiple Giga samples per second). In addition, S&C and most other OFDM synchronisation methods require training symbols which lead to a reduction in the data throughput. Non-data aided algorithms that work blindly without sacrificing system capacity would be very useful in achieving high spectral efficiency.

A number of synchronisation techniques specifically targeting multi-gigabit per second optical OFDM have been developed in recent years [4–9]. Giddings *et al.* [4] proposed superimposing a pattern of DC offset levels on OFDM symbols. The DC levels vary from symbol to symbol in a pattern known to the receiver. The received signal is then correlated with the known pattern, averaged over multiple symbol periods and the correlation output gives peaks indicating the correct symbol boundaries. Bouziane *et al.* presented a method using training symbols and frequency-domain cross-correlation in [6] and another technique based on the standard deviation of the FFT output symbols in [7]. The principle of operation was that in the case of a synchronised system the symbols should be closely clustered and

#203554 - $15.00 USD Received 20 Dec 2013; revised 31 Jan 2014; accepted 31 Jan 2014; published 18 Feb 2014

consequently their standard deviation should be at a minimum. Most recently, we proposed [8] and assessed [9] the performance of a non-data-aided algorithm with low complexity in an optical back-to-back configuration by using the already-existing virtual subcarriers (VSC). VSC are subcarriers that carry no data and usually constitute a small fraction of the FFT output. Similar techniques making use of VSC have been suggested in the past in the context of wireless communications for carrier frequency offset (CFO) estimation [10–13]. These techniques develop a cost function based on VSC and suggest algorithms to optimise it and estimate CFO using *e.g.* a MUSIC-like algorithm [10] or an ESPRIT-like algorithm [11].

The proposed method in this paper investigates the symbol timing offset in optical OFDM and uses the power of VSC (P_{vsc}) as an indicator for the offset. Assuming the system is noise-free, P_{vsc} should be zero if symbol synchronisation is maintained; otherwise, energy from adjacent subcarriers will leak to VSC. Noise in the system will increase P_{vsc} but its value should reach a minimum when synchronisation is achieved. Based on this observation, one can detect the timing offset by monitoring P_{vsc} and determining its minimum.

The algorithm first calculates P_{vsc} for all N possible offset values (where N is the FFT size) and then selects the one that gives minimum P_{vsc} [8]. Here, the correct symbol offset is assumed to be a positive integer between 0 and N-1. This process can be accelerated if a search algorithm like the least-mean-squares is used. The accuracy of the estimation can be improved if P_{vsc} is averaged over multiple symbols. The resulting reduction in digital signal processing (DSP) complexity and bandwidth overhead makes this technique a practical approach in optical OFDM systems. In this paper, we extend the work presented in [9] by experimentally assessing the performance of the method using real-time-generated signals and comparing its performance with that of S&C in optical transmission over 23.3 km of standard single mode fibre (SSMF). The real-time transmitter operates at a bit rate of 30.65 Gb/s, which makes it one of the highest-throughput real-time DD-OFDM systems reported to date.

Several publications have reported real-time implementations of DD-OFDM for next generation PON based on field programmable gate arrays (FPGAs) and digital-to-analogue and analogue-to-digital converters (DAC/ADC) [14–17]. The latest published results include the work of Hugues-Salas *et al.* in which a real-time end-to-end OFDM system with intensity modulation and direct detection (IM/DD) operating at 11.25 Gb/s has been reported [14]. In 2013, the same group demonstrated a dual-band real-time OFDM system with data rates of 20 Gb/s using two independent FPGA-DAC subsystems [15]. The receiver side, which contained one ADC-FPGA pair, received one band at a time. Meanwhile, Cho *et al.* reported a real-time DD-OFDM transceiver operating at 11.52 Gb/s for IM/DD OFDMA-PON systems [16]. More recently, Giddings *et al.* demonstrated a triple sub-band OFDM transceiver with a bitrate of 30 Gb/s [18] and Li *et al.* showed transmission and reception of DD-OFDM signals at 50 Gb/s [19]. This however was achieved with high BER (10^{-2}) and soft decision forward error correction (SD-FEC) was suggested to correct for this. The experiments described in this paper report the real-time generation and transmission of DD 16-level quadrature amplitude modulation (16-QAM) OFDM signals with a bit rate of 30.65 Gb/s using a single FPGA-DAC and transmission over 23.3 km of SSMF with BER less than 10^{-3}. The use of a single band avoids the need for analogue mixers, and multiple DAC/ADCs. The rest of the paper is organized as follows: Section 2 describes the system configuration and experimental setup. Section 3 presents the characterization of the real-time transmitter and transmission results, and section 4 describes a performance comparison between the proposed synchronisation scheme and the Schmidl and Cox algorithm.

2. Experimental setup

A block diagram of the OFDM transmitter DSP is shown in Fig. 1. At each clock cycle, a sequence of 200 bits from a 2^{15} DeBruijn pattern was sent to 16-QAM encoders generating 50 complex symbols. These symbols and their complex conjugates were fed to a 128-point IFFT using the Hermitian symmetry so that the output of the IFFT was real, thus following the discrete multi-tone (DMT) configuration. Both the symbol mapping and the IFFT had 12 bits of resolution. To design the IFFT block, we utilised Spiral, a tool that can automatically

#203554 - $15.00 USD Received 20 Dec 2013; revised 31 Jan 2014; accepted 31 Jan 2014; published 18 Feb 2014

generate hardware and software cores for DSP transforms [20]. Subcarriers located at high frequencies (26 of them) were used as VSC (i.e. they were set to zero and transmitted no data) because they had low signal-to-noise ratio (SNR) due to the roll-off in the system frequency response. These were later used for the proposed VSC synchronisation scheme. The output of the IFFT was then clipped and scaled in order to reduce the peak-to-average power ratio of the signal and match the resolution of the DAC (6 bits). These DSP blocks were implemented on a Xilinx Virtex-5 FPGA board (XC5VFX200T) running at a clock frequency of 156.25 MHz. The transmitter employed 50 data subcarriers all encoded with 16-QAM resulting in a raw data rate of 31.25 Gb/s. An overhead of 1.9% was allocated for channel estimation training symbols; therefore, the net data rate was 30.65 Gb/s (giving a 28.64 Gb/s payload data rate assuming a 7% FEC overhead).

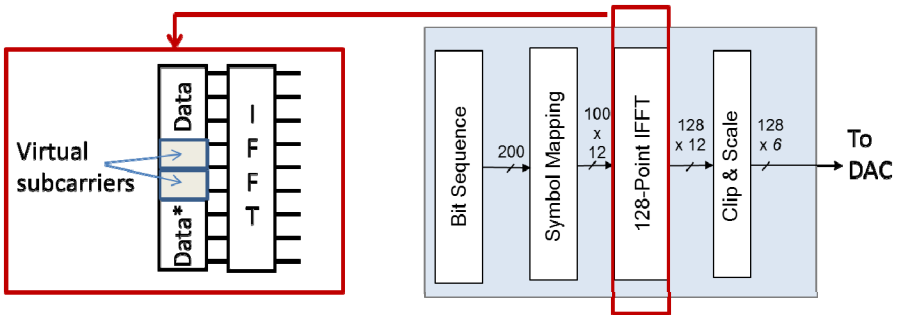

Fig. 1. Block diagram of the transmitter DSP.

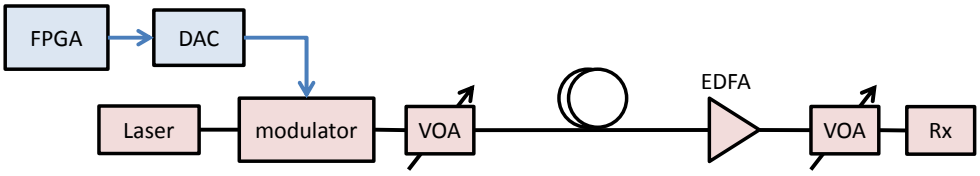

Fig. 2. Experimental system setup. VOA: variable optical attenuator, EDFA: erbium-doped fibre amplifier, Rx: receiver.

As shown in Fig. 2, the output of the FPGA was passed to a DAC (Micram VEGA DAC II) with a sampling frequency of 20 GS/s and a nominal resolution of 6 bits (effective number of bits, ENOB, of 4 at 8 GHz). The output of the DAC was used to drive a Mach-Zehnder modulator to generate the intensity-modulated signal waveform. An external cavity laser (ECL) operating at 1550nm was used as the transmitter optical source, although a source with a wider linewidth would perform equally well since the signals are modulated onto the intensity of the optical field and directly detected with a photodiode. In the optical back-to-back configuration, the output of the modulator was amplified using an erbium-doped fibre amplifier (EDFA) which was operated in saturation with an output power of 18.5 dBm and a noise figure of 4.5 dB. In the transmission experiment, an optical attenuator followed by a span of 23.3 km of SSMF (with 4.5 dB loss) were used between the modulator and the EDFA. The launch power into the fibre was set to 0 dBm. The signal was then attenuated before being received by a Discovery photo-detector (DSC10) followed by an SHF amplifier (SHF806P). A Tektronix digital sampling scope with 50 GS/s sampling frequency and a nominal resolution of 8 bits was used to capture the waveforms. The waveforms were then processed offline using Matlab. The receiver offline DSP included the following blocks: resampling, symbol synchronisation, FFT, channel equalisation, symbol de-mapping, and BER calculation using 1.024×10^5 bits. Resampling was done by down-sampling the received signals and adjusting the phases of the samples until best performance was obtained. The channel frequency response estimation was performed using 10 training symbols in every 512 OFDM symbols, therefore the training symbols overhead was approximately 1.9%.

#203554 - $15.00 USD Received 20 Dec 2013; revised 31 Jan 2014; accepted 31 Jan 2014; published 18 Feb 2014

3. Performance measurements of the real-time transmitter

The received power was varied from −11 dBm to + 3 dBm and BER was calculated by error counting in each case. First, the Schmidl and Cox algorithm was used for symbol synchronisation. Figure 3(a) shows the BER of the system as a function of the received power. The hard decision (HD) FEC limit was assumed to be $3.8\text{x}10^{-3}$ [21] and is indicated in the figure as well. BER is below the FEC limit for received powers greater than or equal to −1 dBm in the back-to-back configuration and + 1 dBm after transmission. There is a penalty of approximately 2 dB caused partly by dispersion, since the OFDM symbols didn't include cyclic prefix in order to save resources and reduce overhead, and partly by additional amplified spontaneous emission (ASE) noise from the optical amplifier. Figures 3(b)–3(e) show example constellation diagrams of the received signals at 2 dBm received power in both cases: back-to-back and 23.3 km SSMF transmission. All subcarriers are plotted together in Figs. 3(b) and 3(c) and only one subcarrier (subcarrier number 10) is plotted in Figs. 3(d) and 3(e).

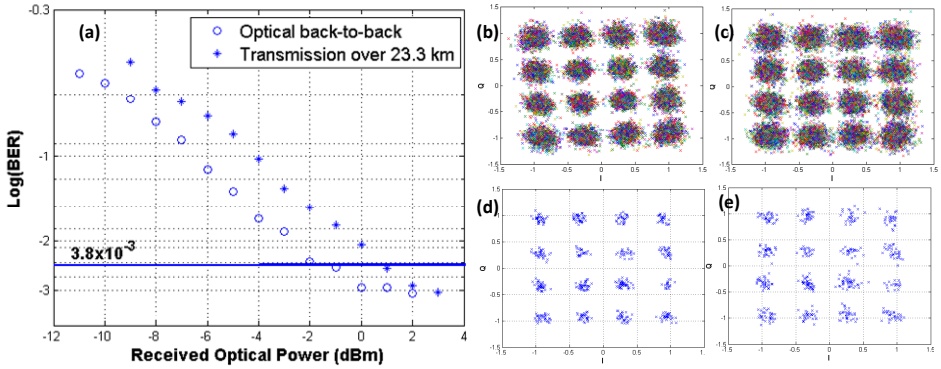

Fig. 3. (a) BER versus received optical power in the optical back-to-back configuration, and after transmission over 23.3 km SSMF. The HD-FEC limit of $3.8\text{x}10^{-3}$ is shown as a straight line. Example constellation diagrams of the received signal at 2 dBm received power, (b) all subcarriers, back-to-back (c) all subcarriers, after 23.3 km transmission, (d) 10th subcarrier only, back-to-back and (e) 10th subcarrier only, 23.3 km transmission.

4. Performance comparison between S&C and the proposed synchronisation method

The Schmidl and Cox (S&C) synchronisation algorithm is a data-aided method that uses training symbols and cross-correlation in the time-domain to detect the timing offset. In [9], we proposed a simpler method which does not rely on training symbols nor on the cyclic prefix, but uses the power of virtual subcarriers instead to perform symbol synchronisation. Here, we assess the performance of the method using the real-time-generated data and compare its performance with that of S&C.

Figure 4(a) illustrates how the power of virtual subcarriers changes as the symbol offset is swept from 0 to 127. This was obtained for the transmission case with 2 dBm received power and 100 averaging symbols (symbols over which the power calculation was averaged). The power profile reaches a minimum at a symbol offset of 110 which is the correct offset. If the number of averaging symbols is decreased as shown in Fig. 4(b), the shape of the power profile becomes noisier but the correct offset is still determined for all cases.

#203554 - $15.00 USD Received 20 Dec 2013; revised 31 Jan 2014; accepted 31 Jan 2014; published 18 Feb 2014

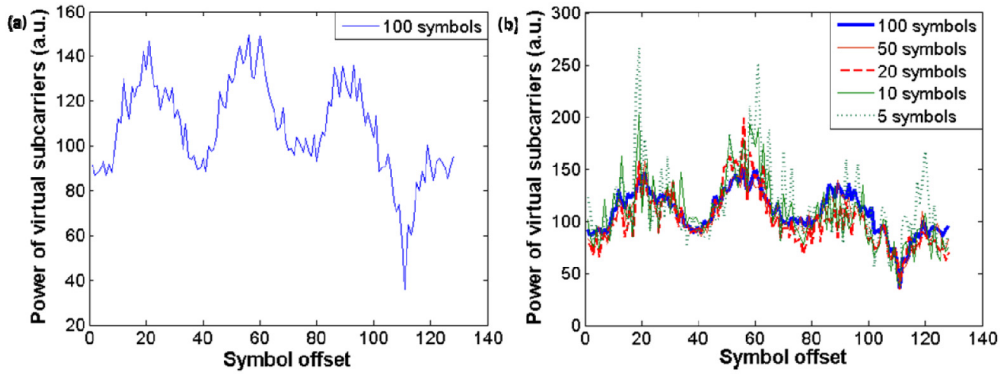

Fig. 4. Power of virtual subcarriers versus symbol offset in the transmission case with 2 dBm received optical power and (a) 100 averaging symbols, (b) different numbers of averaging symbols.

Figures 5 and 6 compare the performance of the proposed method using different numbers of averaging symbols in the optical back-to-back configuration (Fig. 5) and after transmission (Fig. 6). Using 100 symbols, the performance of the proposed method is similar to that of S&C. However, reducing the number of symbols degrades the performance at low received powers. This performance degradation is more pronounced in the transmission case because of the effects of dispersion and additional ASE noise from the optical amplifier. With 10 symbols, the performance of the two methods is the same down to a received power of −7 dBm in the back-to-back-case. This increases to −4 dBm after transmission.

Figure 5(b) shows the minimum received power at which the performance of the proposed method matches that of S&C as a function of the number of symbols over which the metric is averaged. For best performance, 100 symbols need to be used; otherwise, increasing the SNR would improve the robustness of the method at low numbers of symbols. It is worth noting that although the synchronisation speed (the rate at which synchronisation is achieved) reduces in the case of 100 symbols (10 times lower than that of 10 symbols), the circuit complexity remains the same. Figures 5(b) and 6(b) show the trade-off between robustness and synchronisation rate.

In terms of complexity, the proposed method operates at the output of the FFT and calculates the power of virtual subcarriers only requiring 26 complex multipliers and 25 real adders. This represents a small number of operations relative to the rest of the processing in the transceiver. For example, our optimised FFT algorithm requires 166 complex multipliers and 896 complex adders. If S&C is implemented in parallel over $S = 128$ channels, it would require $S = 128$ complex multipliers and $S^2 = 16384$ real adders, although simpler implementations have been suggested *e.g* [22], but with other limitations as explained in that reference. It is worth noting that the S&C algorithm provides information on CFO as well as symbol synchronisation, unlike the proposed algorithm which has not been tested in the presence of CFO because CFO does not arise in DD systems. If a coherent system was considered, then CFO would lead to subcarrier crosstalk and consequently may affect the performance of the proposed synchronisation scheme. In addition, the number of VSCs is a parameter that can be optimised because it gives a trade-off between performance on one side and complexity and bandwidth overhead on the other side (a large number of VSCs improves the synchronisation accuracy but increases the computational complexity and bandwidth overhead). These studies will be subject to future research.

#203554 - $15.00 USD Received 20 Dec 2013; revised 31 Jan 2014; accepted 31 Jan 2014; published 18 Feb 2014

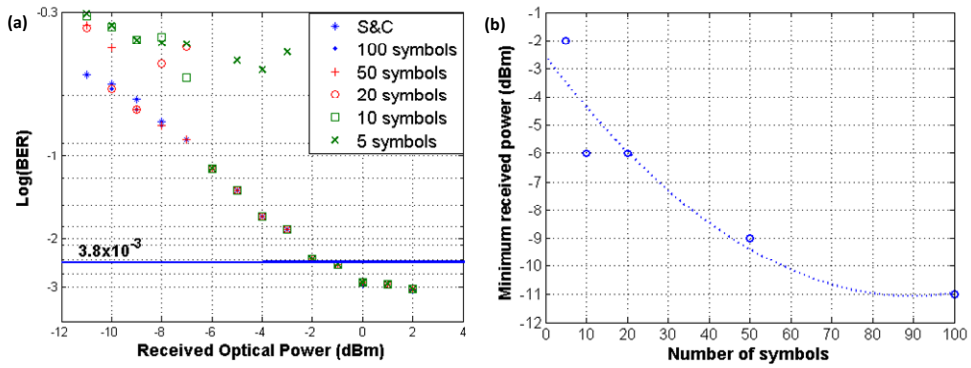

Fig. 5. (a) Performance comparison between Schmidl and Cox algorithm (S&C) and the proposed non-data aided synchronisation method using different numbers of averaging symbols in the optical back-to-back configuration. (b) Minimum received power to match the performance of S&C vs. number of averaging symbols.

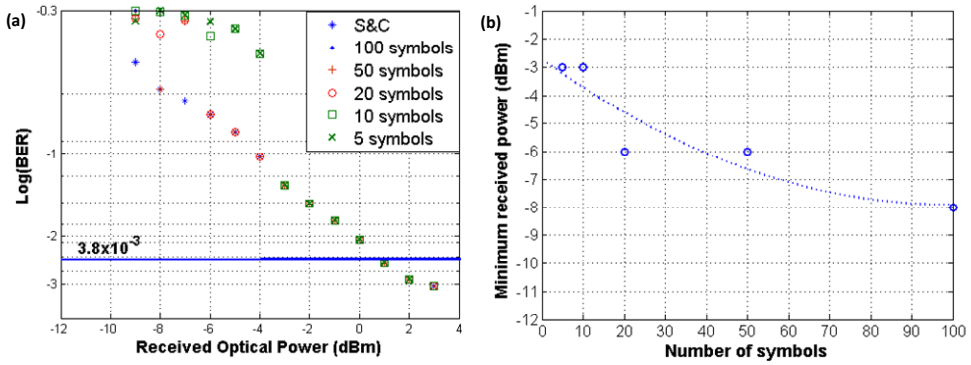

Fig. 6. (a) Performance comparison between Schmidl and Cox algorithm (S&C) and the proposed non-data aided synchronisation method using different numbers of averaging symbols after transmission over 23.3 km SSMF. (b) Minimum received power to match the performance of S&C versus number of averaging symbols.

5. Conclusion

The paper assessed and quantified the performance of a non-data-aided OFDM symbol synchronisation scheme based on virtual subcarriers and compared its performance with that of the Schmidl and Cox algorithm. The experimental setup included an FPGA-based real-time optical OFDM transmitter operating at a bit rate of 30.65 Gb/s in a direct-detection configuration and transmitted over 23.3 km of SSMF achieving BER less than $3.8\text{x}10^{-3}$ for 1 dBm received power. There is a trade-off between the accuracy of the proposed symbol synchronisation technique and its synchronisation rate. Moreover, it exhibits low complexity and bandwidth overhead, which make it suitable for implementation in high speed optical OFDM transceivers. The results presented in the paper show a step forward towards realising low-cost, spectrally-efficient signalling for PON systems, data centres, and back-hauling with 40 Gb/s and 100 Gb/s per wavelength.

Acknowledgments

The work was funded by the UK EPSRC Programme Grant UNLOC EP/J017582/1, the EU ERA- NET + project PIANO + IMPACT, and the EU FP7 ASTRON project (grant agreement no. 318714).

#203554 - $15.00 USD Received 20 Dec 2013; revised 31 Jan 2014; accepted 31 Jan 2014; published 18 Feb 2014